

Strategies for Effective Degradation of Methyl Orange Dye in Aqueous Solution via Electrochemical Treatment with Copper/Graphite Electrodes

Kanayo Oguzie^{1,2*}, John Anyanwu¹, Onyinyechi Enyia², Chikwado Anene¹, Ladislav Vrsalović³, Emeka Oguzie¹

¹ Africa Centre of Excellence in Future Energies and Electrochemical Systems (ACE-FUELS), Federal University of Technology Owerri, P.O.B. 1526, 460113 Owerri, Imo State, Nigeria

² Department of Environmental Management, Federal University of Technology Owerri, P.O.B. 1526, 460113 Owerri, Imo State, Nigeria

³ Faculty of Chemistry and Technology, Department of Electrochemistry and Materials Protection, University of Split, Ruđera Boškovića 35, 21000 Split, Croatia

* Corresponding author, e-mail: kanayo.oguzie@futo.edu.ng

Received: 24 May 2023, Accepted: 08 September 2023, Published online: 04 April 2024

Abstract

This study investigated the electrochemical degradation of methyl orange dye (MO) in aqueous solution using copper/graphite electrodes as anode and cathode respectively. The process parameters such as electrolyte concentrations, current density, pH and temperature were analyzed. The results proved that copper/graphite electrodes were effective for MO degradation and the reaction followed the first-order kinetic model. The degradation efficiency decreased with increasing MO concentration and increased steadily with current density. The pH trend with degradation efficiency was pH 9 (98%) > pH 7 (96%) > pH 3 (77%) after 70 min of electrolysis time, which shows that the alkaline conditions favoured the degradation process. Fourier transform infrared spectroscopy (FTIR) and UV-Vis absorption spectroscopy confirmed the dye degradation process, with the formation of degradation intermediates. The FTIR results revealed that the oxidative degradation of MO may be initiated at the N=N azo bond, which was confirmed by quantum chemical modelling of the electronic structure parameters of MO.

Keywords

methyl orange, electrodes, wastewater treatment, FTIR, electrochemical degradation

1 Introduction

Water pollution is a global environmental issue associated with increasing rates of urbanization and industrialization. Dye wastewaters are usually produced by industrial processes, such as metal plating, paint, pulp and paper, textile, pharmaceutical, petrochemical industries, to mention but a few. The treatment of dye wastewater produced by textile industries has continued to attract much attention [1–3], due to their persistence in the environment, and conventional treatment methods are often insufficient to remove them completely from the environment [4, 5]. Electrochemical oxidation is now considered a promising technique for the degradation of persistent organic pollutants present in wastewater. The technique is proving attractive due to its cost-effectiveness, high efficiency,

environmental compatibility, versatility, simplicity of deployment and ease of operation [6–11].

Electrochemical oxidation employs either, indirect or direct oxidation processes, or both, during electrolysis, to degrade a wide range of organic contaminants and decontaminate different environmental matrices (soil, water and even air). Anode materials play a key role in electrochemical oxidation, influencing process efficiency as well as system integrity [12, 13]. Electrochemical oxidation has been found effective for dye degradation [14, 15] and has also demonstrated that organic pollutants can be completely mineralized, forming CO₂ and H₂O as end products [16].

Methyl orange (MO) is a water-soluble azo dye, commonly used as a dye in the food, paper and leather textile

industries [1]. The presence of the sulphonic group and the stable double bond N=N in the structure, imparts acidic properties to the dye. The release of MO containing wastewater into the environment without proper treatment has pronounced adverse environmental and health effects, including mutagenic and carcinogenic consequences [17, 18]. Therefore, the development of techniques for the degradation of MO remains an R&D priority. Yang et al. [19] studied the electrochemical degradation of methyl orange wastewater by Nb/PbO₂ electrodes and obtained a degradation efficiency of 99.6%. Yusuf et al. [20] observed an efficiency of almost 100% within 13 min for the degradation of methyl orange using a novel polymer disk electrode. Chaúque and co-workers [5] used Fe/Ag nanoparticles immobilized on polyacrylonitrile nanofibers for the MO removal, using EDTA chelating agents, and obtained >96% removal efficiency.

The choice of electrode material plays an important role in achieving high efficiencies in the oxidative degradation of pollutants. In this study, copper and graphite are used as anode and cathode materials for the electrochemical degradation of methyl orange in an environment. The optimization of the electrochemical degradation of methyl orange was achieved by evaluating the influence of several process parameters such as electrolyte concentration.

2 Methodology

2.1 Chemicals and reagents

Methyl orange (MO) obtained from Aldrich was used to prepare a test solution at a concentration of 15 mg/L. Potassium chloride (Sinopharm, China) was used as a supporting electrolyte. Sulphuric acid and sodium hydroxide (Sinopharm, China) were used for pH adjustment. All chemicals were analytical reagent grade and were used without further purification.

2.2 Dye degradation experiments

Electrochemical degradation of MO solution was carried out in an electrolytic cell of 500 cm³ capacity, with a thermostatic magnetic stirrer (Hanchen, ZHU-245, China). Copper and graphite plates with dimensions 100 × 30 × 2 mm were used as anode and cathode, respectively, and were connected to a digital DC power supply (MCH-K305D, China). The supporting electrolyte KCl was added to the dye solution prior to electrolysis. 1 M H₂SO₄ or 0.1 M NaOH was used for the pH adjustment of the dye solution. For the experiment, MO was mixed with the required amount of the electrolyte. The electrodes were connected to the DC power

supply and the current density was set to the desired value. Samples were retrieved at 10 min intervals during the electrolysis process, up to 70 min and then sent for analysis. Experimental variables included initial solution pH (3, 9 and 11), current density (15 mA/cm²–75 mA/cm²), temperature ($T = 303, 318$ and 333 K) and electrolyte concentration (0.5–1.5 M). All experiments were performed in triplicate, and the standard deviation ranged from 0.25 to 2.43%.

2.3 Analytical procedure

The concentrations of MO before and after the electrolytic degradation experiments were determined using a UV-Vis spectrophotometer Lasany (LI-722), India. The degradation efficiency (DE) was calculated using the following relationship:

$$DE\% = \frac{C_i - C_f}{C_i} \times 100, \quad (1)$$

where C_i is the initial dye concentration (mg/L) and C_f is the dye concentration (mg/L) after electrolysis for a time interval t .

Time evolution of the MO degradation profile was monitored by full wavelength scanning experiments using a Shimadzu UV-3600 Plus UV-Vis-NIR spectrophotometer, Japan at a maximum wavelength ($\lambda_{\max} = 470$ nm) for dye solutions. Also, the degradation-induced changes in functional groups on MO and its degradation intermediates were monitored using a Spectrum 2 Fourier transform infrared spectrophotometer (FTIR, Perkin Elmer).

2.4 Quantum chemical computations

Computations were performed using the density functional theory (DFT) electronic structure program DMol3 included in the Material Studio software (BIOVIA Materials Studio Academic Research Suite (Product No: 5CB-LUR), France).

3 Results and discussion

3.1 Degradation profile of methyl orange dye

UV-Vis absorption spectroscopy has been used to monitor the degradation process of MO with time. The maximum absorption wavelength of MO in the visible range is 470 nm. Fig. 1 presents the degradation profile of MO, with the maximum absorption peak at 470 nm, which decreased steadily in intensity with the progress of degradation. The disappearance of the peak was observed after 40 min, indicating complete decolorization of the MO contaminated water by the copper anode and graphite cathode.

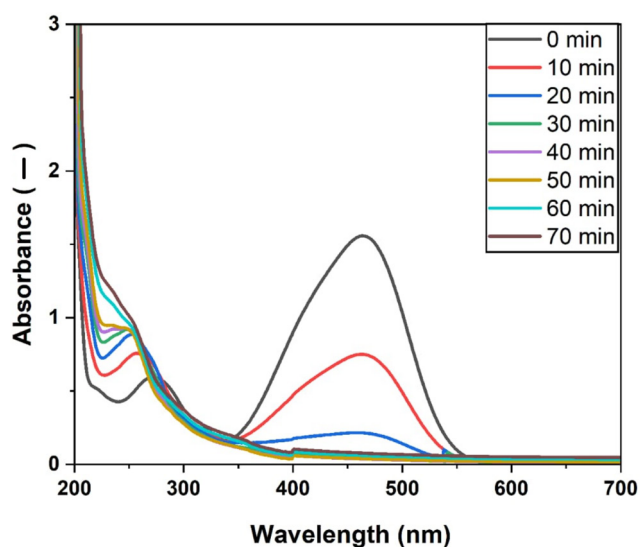


Fig. 1 Full wavelength scanning of degradation behaviour of MO with time

3.2 Effect of supporting electrolyte

Electrolytes contain ions that increase the conductivity of a solution, making them electrically conductive, thereby providing support for the exchange of electrons between the anode and the cathode, which can promote both direct and indirect oxidation of contaminants. Electrolytes are essential additives in the electrolysis of poorly conducting organic species like organic dyes. Accordingly, the influence of different concentrations of potassium chloride on the decolorization of MO-containing wastewater was investigated in this study.

Fig. 2 illustrates the effects of different KCl concentrations on the decolorization efficiency of MO. The results clearly show that the decolorization efficiency increases with KCl concentration, with an optimal effect observed for 1 M KCl. At low KCl concentrations (0.05–0.5 M), a steady linear increase in decolorization efficiency is observed, within the time interval studied. At a KCl concentration of

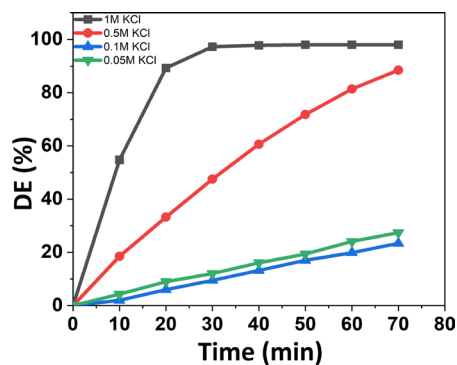
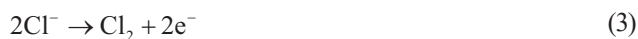


Fig. 2 Effect of KCl electrolyte on decolorization efficiency of MO (Dye concentration = 15 mg/L, $T = 301$ K, voltage (U) = 25 V, current density = 75 mA/cm²)

1.0 M, the linear increase in efficiency with time occurred rapidly, and after 30 minutes a stable decolorization state was reached, with a decolorization efficiency of 98%.

The KCl electrolyte, not only increases the conductivity of the solution, but also generates strongly oxidizing chlorinated species (Cl_2 , HOCl, and OCl⁻), that result from oxidation of the chloride anion (Eqs. (2)–(5)). These species promote rapid degradation of the pollutants [21]. Accordingly, the high degradation rate at higher Cl⁻ concentration is attributed to the formation of a larger concentration of active oxidizing chlorinated species.



3.3 Effect of current density

In electrochemical oxidation processes, current density is one of the most important factors responsible for initiating and maintaining electron flow through the electrochemical cell. Current density influences both electron transfer and the generation of active species, which directly affects organic pollutants removal rates. The effect of current density on MO decolorization efficiency was investigated and the results are shown in Fig. 3. A trend of increasing decolorization efficiency with both current density and time is obvious from Fig. 4. The highest degradation efficiency of 98% was obtained at a high current density of 75 mA/cm² in 70 minutes.

Increasing the current density of an electrolytic process should enhance numerous individual background processes. For instance, higher current densities increase

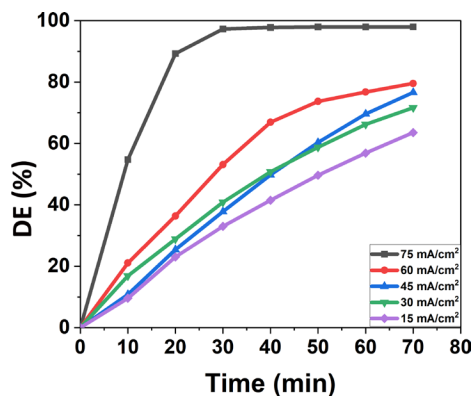


Fig. 3 Effect of current density degradation efficiency on MO (Dye concentration = 15 mg/L, $T = 301$ K, $U = 25$ V, electrolyte = 1 M KCl)

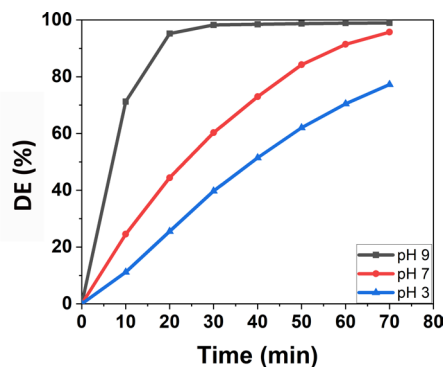


Fig. 4 Effect of Initial pH on degradation of methyl orange (dye concentration = 15 mg/L, $T = 301$ K, $U = 25$ V, electrolyte = 1 M KCl)

the rate of transport of electroactive species towards the electrodes and as also increase the rates of electron transfer reactions at the interface, resulting in a net increase in the rates of electrochemical processes. Moreover, higher current densities should also increase the generation rates of highly oxidizing chlorinated species responsible for the oxidative degradation of MO [22, 23]. Wang et al. [24] studied the electrochemical oxidation of methyl orange with Magnéli phase Ti_4O_7 anode and observed that the degradation of MO was current density dependent, reaching 99% removal rate after 30 min when the current density increased. Yang et al. [19] observed the MO removal efficiency increased with an increase in current density using a Nb/PbO₂ electrode. This behaviour was also attributed to the generation of more oxidising free species, such as peroxodisulfates or hydroxyl radicals. According to Yusuf et al. [20], the slow degradation of MO at lower current results from the associated reduction in the reaction flux.

3.4 Influence of pH on the degradation of MO

The physicochemical properties of the wastewater produced by different industries indirectly change the pH of the wastewater. Dilute H₂SO₄ and NaOH solutions were used for pH adjustment. To investigate the influence of different pH values on the electrochemical degradation of MO, the experiments were performed at acidic (pH 3), neutral (pH 7) and basic (pH 9) conditions.

Fig. 4 shows that the pH degradation efficiency of MO follows the trend pH 9 (98% @ 40 min) > pH 7 (96% @ 70 min) > pH 3 (77% @ 70 min) after 70 minutes of electrolysis time. The result obtained shows that alkaline condition were the most favourable for the degradation of MO.

Some authors have proved that the anodic oxidation of organic pollutants either favours the acidic or the alkaline conditions in their studies [25]. Both researchers [22, 26] had similar findings to our results in their works. These

results can be ascribed to the accumulation of OH⁻ on the surface of the anode under alkaline conditions, which can prevent the oxidation of the anionic organic matter.

3.5 Effect of temperature

Temperature plays an important role in the rate of chemical and electrochemical reactions. In electrochemical degradation processes, the effect of temperature depends on the electrode materials used, the pollutant to be degraded and the current density applied. Fig. 5 shows the effects of different temperatures (303, 318 and 333 K) on the electrochemical degradation of MO. Very little variation in decolorization efficiency over time is observed at the different temperatures. The system at 318 K was the first to achieve optimal and steady state efficiency, while the system at 333 K was the last. The optimum efficiencies at the different temperatures also followed an almost insignificant trend; 303 K (99%) > 318 K (98%) > 333 K (97%).

Our results imply that an increase in temperature does not increase the rate of the degradation process, as would be expected for electrochemical processes, but rather leads to a very small decrease in MO decolorization efficiency. Similar observations have been reported by [27, 28]. This implies that some other background processes may counteract the expected increase in reaction kinetics with increasing temperature. In this context, it has been shown that the reactive chlorinated species responsible for contaminant oxidation are readily decomposed when the process temperature is increased. This is particularly true for HOCl and Cl₂, which are gaseous species.

3.6 Degradation kinetics of methyl orange

The reaction order for the degradation of MO was determined by the integral method and is consistent with the first-order reaction model, as shown by the linear plots of

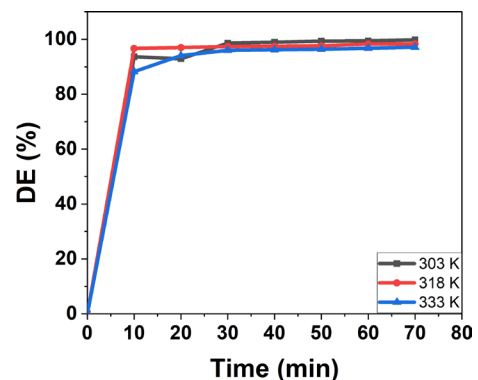


Fig. 5 Effect of temperature on degradation efficiency for MO (dye concentration = 15 mg/L, $U = 25$ V, electrolyte = 1 M KCl)

$\ln(A/A_0)$ vs time in Fig. 6. The first-order kinetic equation is given by [20]:

$$\ln(A/A_0) = -k \times t, \quad (6)$$

where A_0 is the initial MO absorbance, A is the MO absorbance at time t , and k is the electrochemical degradation rate constant for MO.

3.7 FTIR analysis

MO degradation was further investigated by FTIR, to monitor the evolution of the functional groups as a function of degradation time. Fig. 7 shows the FTIR spectra for MO before degradation (a) and after degradation for 45 min (b) and 70 min (c). The electrochemical degradation process resulted in the disappearance of several characteristic peaks in the MO spectra. These include the bands for phenyl at 1596 and 1447 cm^{-1} , band at 1358 cm^{-1} associated with aromatic C–N bonds and the N=N azo bond at 1436 cm^{-1} . These observations imply that the progressive electrochemical degradation leads to the breakup of the phenyl ring, as well as the Ar–C–N and azo bonds. Obviously, the cleavage of the azo bond would initiate the disintegration of the azo chromophore and subsequent decolourization of MO. Other bands that disappeared after degradation include a series of bands from 1170 to 813 cm^{-1} , such as that of sulfonyl group at 1043 cm^{-1} , C–H bonds of di-substituted benzene at 813 cm^{-1} . The band at 574 cm^{-1} shifted to higher wavenumbers at 613 and 624 cm^{-1} , suggesting that the species bearing the functional group underwent degradation, resulting in increased vibration frequencies. After

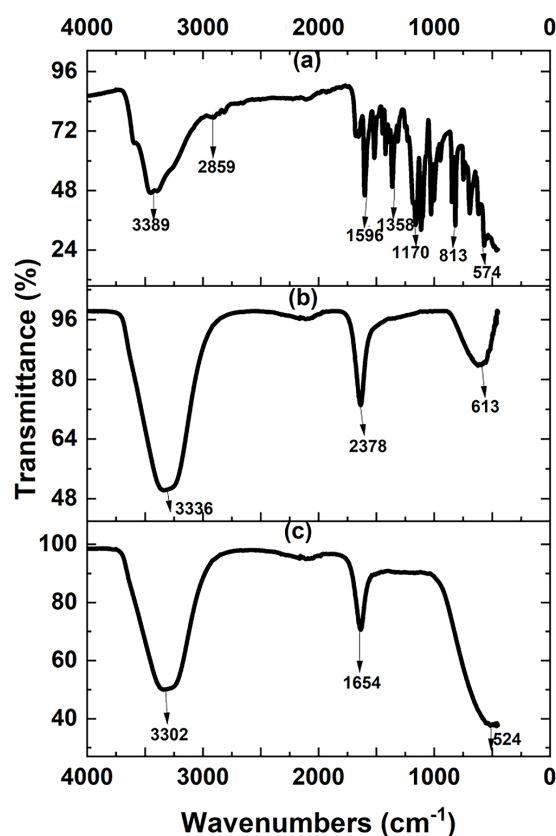


Fig. 7 FTIR spectra of the MO dye solution: (a) before degradation ($t = 0$ min), (b) after 45 min (c) after 70 min of degradation

the degradation process, some newly formed bands were also observed. The new but short-lived band appearing after 45 min at 2378 cm^{-1} indicates the possible presence of a C–C or C–N triple bond. The new band at 1654 cm^{-1} can be ascribed to the C=O carbonyl group.

The FTIR results show clearly that the electrochemical degradation of MO proceeded via oxidative attachment to several functional groups in the dye molecule, including the N=N azo bond, the C–N bond, the phenyl group, as well as the sulfonyl group, producing several degradation intermediates. Du et al [29] reported similar FTIR spectra for the chloride-enhanced electrochemical degradation of MO using RuO_x–PdO/Ti anodes.

3.8 Quantum chemical computation

Our FTIR results suggest that the N=N azo bond, the C–N bond, and/or the phenyl group are possible sites for the onset of oxidative degradation of MO. In fact, based on GC–MS analysis of MO degradation intermediates, Du et al. [29], proposed a degradation mechanism that occurs via attack on the N=N azo bond. We have thus undertaken electronic structure modelling of the MO molecule to map the reactivity of different sites to

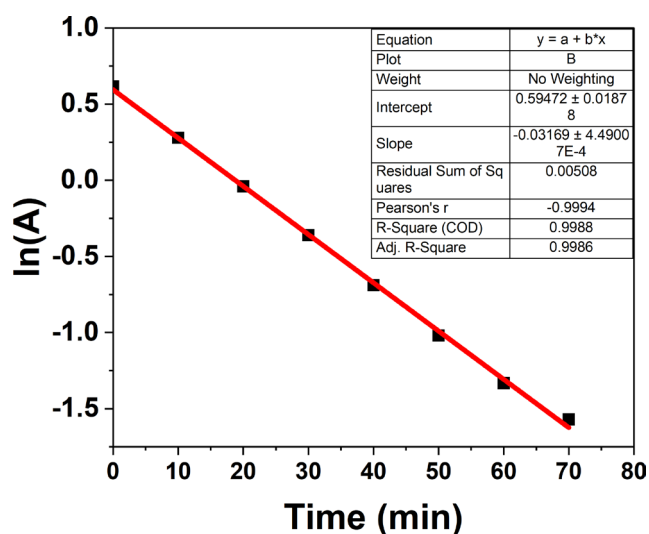


Fig. 6 First order kinetic plot the electrochemical degradation of MO (dye concentration = 15 mg/L, $T = 301$ K, $U = 25$ V, current density = 75 mA/cm^2 , pH = 7, electrolyte = 0.5 M KCl)

oxidizing species. Details of the computational protocol are reported elsewhere [30]. The reactivity descriptors of interest include the frontier molecular orbitals and the Fukui indices (FI) for electrophilic (F^-) and radical (F^0) attacks. The optimized structure and Fukui functions of the MO molecule are illustrated in Fig. 8 and the calculated Fukui indices for the atoms in the MO molecule are given in Table 1, in terms of Mulliken (Mullik) and Hirshfeld (Hirshfld) population analyses.

To investigate the plausible degradation mechanisms, the degradation intermediates identified based on the azo $N=N$ bond cleavage were further subjected to quantum chemical computations, to determine their theoretical enthalpies of formation and relative stabilities. Fig. 9 shows the electronic structure models like total electron density, HOMO (highest occupied molecular orbital), LUMO (lowest unoccupied molecular orbital), total electron density and enthalpies of formation of MO and the selected degradation intermediates from the azo $N=N$ bond cleavage, as reported by [28, 31, 32]. Species with more positive ΔE values show a greater tendency to lose electrons and are therefore more susceptible to attack by oxidizing species. The ΔE values ranged from 1.69 (MO) to 1.71 (cyclohexa-2,5-diene-1,4-dione), and 3.68 (sulfanilic acid), to 4.65 (benzenesulfonic acid). Interestingly, full UV wavelength scanning of the degradation profile of MO revealed absorption maxima corresponding to cyclohexa-2,5-diene-1,4-dione and sulfanilic acid. Similarly, species with more positive enthalpies of formation would be more unstable and more prone to undergo side reactions and further degradation. The more stable degradation intermediates include sulfanilic acid ($\Delta H_f = -141.9$ kcal/mol), benzenesulfonic acid ($\Delta H_f = -142.5$ kcal/mol), and oxalic acid ($\Delta H_f = -192.0$ kcal/mol). According to Gómez-Obando et al. [31], these compounds represent the most common MO degradation products, which further decompose into other smaller compounds and are eventually mineralized to carbon dioxide and water.

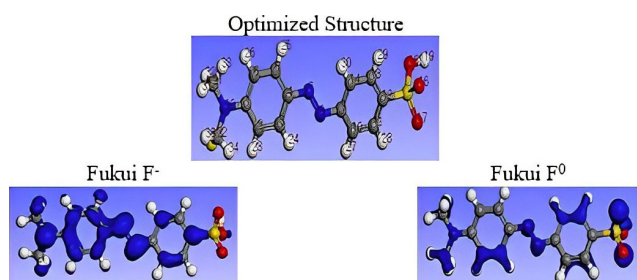


Fig. 8 Optimized structure and Fukui functions of MO molecule

Table 1 Fukui indices for electrophilic attack on MO

Atom	(Fukui(-))		Atom	(Fukui(0))	
	Mullik	Hirshfld		Mullik	Hirshfld
C(1)	0.037	0.034	C(1)	0.026	0.035
C(2)	0.037	0.042	C(2)	0.048	0.048
C(3)	0.036	0.042	C(3)	0.023	0.035
C(4)	0.039	0.048	C(4)	0.061	0.064
C(5)	0.03	0.04	C(5)	0.024	0.038
C(6)	0.041	0.044	C(6)	0.061	0.059
N(7)	0.044	0.062	N(7)	0.064	0.085
N(8)	0.062	0.071	N(8)	0.025	0.034
N(9)	0.072	0.080	N(9)	0.061	0.067
C(10)	0.016	0.027	C(10)	0.01	0.02
C(11)	0.029	0.035	C(11)	0.028	0.031
C(12)	0.019	0.024	C(12)	0.013	0.018
C(13)	0.027	0.035	C(13)	0.024	0.03
C(14)	0.014	0.022	C(14)	0.012	0.018
C(15)	0.038	0.037	C(15)	0.029	0.03
S(16)	0.009	0.011	S(16)	0.005	0.009
O(17)	0.014	0.014	O(17)	0.011	0.01
O(18)	0.012	0.012	O(18)	0.005	0.01
O(19)	0.016	0.016	O(19)	0.023	0.021
Na(20)	0.006	0.006	Na(20)	0.005	0
C(21)	-0.012	0.018	C(21)	-0.015	0.024
C(22)	-0.012	0.018	C(22)	-0.013	0.024
H(23)	0.033	0.02	H(23)	0.036	0.023
H(24)	0.04	0.024	H(24)	0.038	0.021
H(25)	0.039	0.023	H(25)	0.039	0.022
H(26)	0.033	0.02	H(26)	0.039	0.025
H(27)	0.032	0.018	H(27)	0.026	0.015
H(28)	0.021	0.012	H(28)	0.017	0.01
H(29)	0.021	0.012	H(29)	0.017	0.01
H(30)	0.033	0.02	H(30)	0.026	0.015
H(31)	0.021	0.013	H(31)	0.027	0.016
H(32)	0.034	0.022	H(32)	0.046	0.03
H(33)	0.033	0.021	H(33)	0.043	0.028
H(34)	0.034	0.021	H(34)	0.043	0.028
H(35)	0.034	0.022	H(35)	0.045	0.029
H(36)	0.021	0.013	H(36)	0.027	0.016

3.9 Energy consumption

Energy consumption is an important factor to consider when determining the feasibility of electrochemical degradation processes on a commercial scale. The estimated energy consumption during MO degradation was calculated using the relationship in Eqs. (6) [33, 34]:

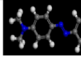
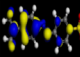
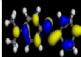
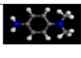
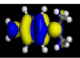
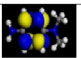
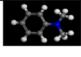
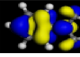
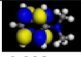
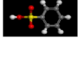
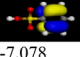
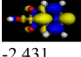
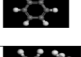

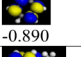
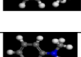
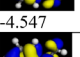
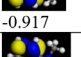
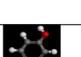
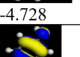
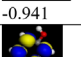
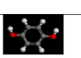
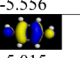
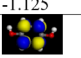
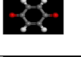
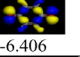
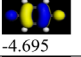
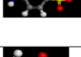
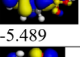
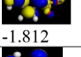

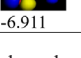
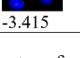
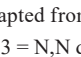
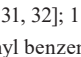
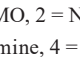
Compound	Structure	HOMO E _{HOMO} (eV)	LUMO E _{LUMO} (eV)	ΔE eV	ΔH _r kcal/mol
MO				1.69	-51.6
		-5.193	-3.506		
N,N dimethyl-p-phenyldiamine				3.20	17.7
		-4.159	-0.962		
N,N dimethyl benzeneamine				3.64	24.2
		-4.567	-0.932		
Benzenesulfonic acid				4.65	-142.5
		-7.078	-2.431		
Phenylamine				3.83	11.4
		-4.723	-0.890		
N,N-dimethylaniline				3.63	24.1
		-4.547	-0.917		
N-methylaniline				3.79	16.5
		-4.728	-0.941		
Phenol				4.43	-30.1
		-5.556	-1.125		
Benzene-1,4 diol				3.80	-77.9
		-5.015	-1.212		
Cyclohexa-2,5-diene-1,4-dione				1.71	-38.3
		-6.406	-4.695		
Sulfanilic acid				3.68	-141.9
		-5.489	-1.812		
Oxalic acid				3.50	-192.0
		-6.911	-3.415		

Fig. 9 Electronic structure models and parameters for MO degradation products as adapted from [29, 31, 32]; 1 = MO, 2 = N,N dimethyl-p-phenyldiamine, 3 = N,N dimethyl benzeneamine, 4 = benzenesulfonic acid, 5 = phenylamine, 6 = N,N-dimethylaniline, 7 = N-methylaniline, 8 = phenol, 9 = benzene-1,4 diol, 10 = cyclohexa-2,5-diene-1,4-dione, 11 = sulfanilic acid, 12 = oxalic acid

$$\text{Energy consumption (kWh)} = \frac{P(W) \times t(h)}{V_{sol} (dm^3)}, \quad (7)$$

where:

$$P(W) = I(A) \times E(V). \quad (8)$$

In Eq. (8) P is the power of the electrochemical cell in Watts (W); t , is the electrolysis time in hours (h); V_{sol} is the volume of treated solution in cubic decimetres (dm^3); I is the current in ampere (A) and U is the voltage in volt (V). The economic feasibility of mineralizing of MO using Cu at the anode and graphite at the cathode as electrodes was shown in Table 2.

As shown in Table 2, energy consumption increased with degradation time for each applied current and increased with increasing current for each time interval. Accordingly, the highest electrical energy consumption (291.67 kWh/ dm^3) was obtained after a degradation time of 70 min at 75 mA/ mm^2 , with a 98% degradation efficiency. However, the optimum degradation (98%) was reached

Table 2 Electrical energy input for degradation of CV

Current (A)	Voltage (V)	Time (h)	Energy consumption (kWh/ m^3)
1	25	0.33	16.67
		0.67	33.33
		1.17	58.33
2	25	0.33	33.33
		0.67	66.67
		1.17	116.67
3	25	0.33	50.00
		0.67	100.00
		1.17	175.00
4	25	0.33	66.67
		0.67	133.33
		1.17	233.33
5	25	0.33	83.33
		0.67	166.67
		1.17	291.67

after just 40 min at high current density, corresponding to an energy consumption of 166.67 kWh/ m^3 . This is less than the 233.33 kWh/ m^3 required for 70 min degradation at a lower current density of 60 mA/ mm^2 , with an 75% efficiency. Zhou et al. [25] observed that the energy consumption is closely related to the activity of the electrode and the structure of the contaminant. The conductivity of the electrolytic media and the energy consumption of the electrochemical process can be affected by the concentration of the supporting electrolyte.

4 Conclusion

In this work, a copper/graphite electrode was used at the anode and cathode for the electrochemical degradation of methyl orange (MO) in aqueous solution. The operating parameters for the degradation of MO were improved. Increasing the electrolyte concentration of KCl leads to an increase in the decolourization efficiency of 98% after 30 min of electrolysis time. It was observed that a higher current density of 75 mA/ cm^2 increases the transport rate of electroactive species to the electrodes and also the rates of electron transfer reactions at the interface, leading to an increase in the rates of electrochemical degradation processes by 98%. A higher degradation efficiency was observed at pH 9, compared to pH 3 with 98% and 77% respectively. The FTIR results presented in this study showed the disappearance of the characteristic peaks of MO such as phenyl group, aromatic C–N bonds and the N=N azo bond. The highest energy consumption after 70 min was reached at 291.67 kWh/ m^3 .

Acknowledgement

Financial support from the World Bank Africa Centres of Excellence for Impact (ACE Impact) Project (NUC/ES/507/1/304).

References

- [1] Hieu, V. Q., Phung, T. K., Nguyen, T. Q., Khan, A., Doan, V.D., Tran, V. A., Le V. T. "Photocatalytic degradation of methyl orange dye by $\text{Ti}_3\text{C}_2\text{eTiO}_2$ heterojunction under solar light", *Chemosphere*, 276, 130154, 2021.
<https://doi.org/10.1016/j.chemosphere.2021.130154>
- [2] Sun, L., Wang, C., Ji, M., Kong, X. "Treatment of mixed chemical wastewater and the agglomeration mechanism via an internal electrolysis filter", *Chemical Engineering Journal*, 215–216, pp. 50–56, 2013.
<https://doi.org/10.1016/j.ccej.2012.11.008>
- [3] Zhu, C., Jiang, C., Chen, S., Mei, R., Wang, X., Cao, J., Ma, L., Zhou, B., Wei, Q., Ouyang, G., Yu, Z., Zhou, K. "Ultrasound enhanced electrochemical oxidation of Alizarin Red S on boron doped diamond (BDD) anode: Effect of degradation process parameters", *Chemosphere*, 209, pp. 685–695, 2018.
<https://doi.org/10.1016/j.chemosphere.2018.06.137>
- [4] Cotillas, S., Llanos, J., Canizare, P., Clematis, D., Cerisola, G., Rodrigo, M. A., Panizza, M. "Removal of Procion Red MX-5B dye from wastewater by conductive-diamond electrochemical oxidation", *Electrochimica Acta*, 263, pp. 1–7, 2018.
<https://doi.org/10.1016/j.electacta.2018.01.052>
- [5] Eutílerio, F. C., Chaúque, E. F. C., Ngilaa, J. C., Rayc, S. C., Ndlwana, L. "Degradation of methyl orange on Fe/Ag nanoparticles immobilized on polyacrylonitrile nanofibers using EDTA chelating agents", *Journal of Environmental Management*, 236, pp. 481–489, 2019.
<https://doi.org/10.1016/j.jenvman.2019.02.023>
- [6] Can, W., Yao-Kun, H., Qing, Z., Min, J. "Treatment of secondary effluent using a three-dimensional electrode system: COD removal, biotoxicity assessment, and disinfection effects", *Chemical Engineering Journal*, 243, pp. 1–6, 2014.
<https://doi.org/10.1016/j.ccej.2013.12.044>
- [7] Salazar, C., Contreras, N., Mansilla, H. D., Yanez, J., Salazar, R. "Electrochemical degradation of the antihypertensive losartan in aqueous medium by electro-oxidation with boron-doped diamond electrode", *Journal of Hazardous Material*, 319, pp. 84–92, 2016.
<https://doi.org/10.1016/j.jhazmat.2016.04.009>
- [8] Shih, Y. J., Huang, Y. H., Huang, C. P. "Oxidation of ammonia in dilute aqueous solutions over graphite-supported alpha- and beta-lead dioxide electrodes ($\text{PbO}_2@G$)", *Electrochimica Acta*, 257, pp. 444–454, 2017.
<https://doi.org/10.1016/j.electacta.2017.10.060>
- [9] Shin, Y.-U., Yoo, H.-Y., Ahn, Y.-Y., Kim, M. S., Leed, K., Yu, S., Lee, C., Cho, K., Kim H.-I., Lee, J. "Electrochemical oxidation of organics in sulfate solutions on boron-doped diamond electrode: Multiple pathways for sulfate radical generation", *Applied Catalysis B: Environmental*, 254, pp. 156–165, 2019.
<https://doi.org/10.1016/j.apcatb.2019.04.060>
- [10] Tien, T. T., Luu, T. L. "Electrooxidation of tannery wastewater with continuous flow system: Role of electrode materials", *Environmental Engineering Resource*, 25(3), pp. 324–334, 2020.
<https://doi.org/10.4491/eer.2018.349>
- [11] Radjenovic, J., Sedlak, D. L. "Challenges and Opportunities for Electrochemical Processes as Next-Generation Technologies for the Treatment of Contaminated Water", *Environmental Science & Technology*, 49(19), pp. 11292–11302, 2015.
<https://doi.org/10.1021/acs.est.5b02414>
- [12] Bian, X., Xia, Y., Zhan, T., Wang, L., Zhou, W., Dai, Q., Chen, J. "Electrochemical removal of amoxicillin using a Cu doped PbO_2 electrode: Electrode characterization, operational parameters optimization and degradation mechanism", *Chemosphere*, 233, pp. 762–770, 2019.
<https://doi.org/10.1016/j.chemosphere.2019.05.226>
- [13] Duan, X. Y., Xu, F., Wang, Y. N., Chen, Y. W., Chang, L. M. "Fabrication of a hydrophobic SDBS- PbO_2 anode for electrochemical degradation of nitrobenzene in aqueous solution", *Electrochimica Acta*, 282, pp. 662–671, 2018.
<https://doi.org/10.1016/j.electacta.2018.06.098>
- [14] Yu, D., Cui, J., Li, X., Zhang, H., Pei, Y. "Electrochemical treatment of organic pollutants in landfill leachate using a three-dimensional electrode system", *Chemosphere*, 243, 12543, 2020.
<https://doi.org/10.1016/j.chemosphere.2019.125438>
- [15] Guenfoud, F., Mokhtari, M., Akrouit, H. "Electrochemical degradation of malachite green with BDD electrodes: Effect of electrochemical parameters", *Diamond and Related Materials*, 46, pp. 8–14, 2014.
<https://doi.org/10.1016/j.diamond.2014.04.003>
- [16] Ansari, A., Nematollahi, D. "Convergent paired electrocatalytic degradation of p-dinitrobenzene by $\text{Ti/SnO}_2\text{-Sb}/\beta\text{-PbO}_2$ anode. A new insight into the electrochemical degradation mechanism", *Applied Catalysis B: Environmental*, 261, 118226, 2020.
<https://doi.org/10.1016/j.apcatb.2019.118226>
- [17] Singh, S., Lo, S. L., Srivastava, V. C., Hiwarkar, A. D. "Comparative study of electrochemical oxidation for dye degradation: Parametric optimization and mechanism identification", *Journal of Environmental Chemical Engineering*, 4(3), pp. 2911–2921, 2016.
<https://doi.org/10.1016/j.jece.2016.05.036>
- [18] Zhang, S. J., Yu, H. Q., Zhao, Y. "Kinetic modelling of the radiolytic degradation of acid Orange 7 in aqueous solutions", *Water Research*, 39(5), pp. 839–846, 2005.
<https://doi.org/10.1016/j.watres.2004.12.004>
- [19] Yang, H., Liang, J., Zhang, L., Liang, Z. "Electrochemical Oxidation Degradation of Methyl Orange Wastewater by Nb/PbO_2 Electrode", *International Journal of Electrochemical Science*, 11, pp. 1121–1134, 2016. [online] Available at: <http://www.electrochemsci.org/papers/vol11/110201121.pdf> [Accessed: 24 April 2023]

- [20] Yusuf, H. A., Redha, Z. M., Baldock, S. J., Fielden, P. R., Goddard, N. J. "An analytical study of the electrochemical degradation of methyl orange using a novel polymer disk electrode", *Microelectronic Engineering*, 149, pp. 31–36, 2016.
<https://doi.org/10.1016/j.mee.2015.09.003>
- [21] Wang, Y., Chen, M., Wang, C., Meng, X., Zhang, W., Chen, Z., Crittenden, J. "Electrochemical degradation of methylisothiazolinone by using Ti/SnO₂-Sb₂O₃/α, β-PbO₂ electrode: Kinetics, energy efficiency, oxidation mechanism and degradation pathway", *Chemical Engineering Journal*, 374, pp. 626–636, 2019.
<https://doi.org/10.1016/j.cej.2019.05.217>
- [22] Gui, L., Peng, J., Li, P., Peng, R., Yu, P., Luo, Y. "Electrochemical degradation of dye on TiO₂ nanotube array constructed anode", *Chemosphere*, 235, pp. 1189–1196, 2019.
<https://doi.org/10.1016/j.chemosphere.2019.06.170>
- [23] Wang, C., Yu, Y., Yin, L., Niu, J., Hou, L.-A. "Insights of ibuprofen electro-oxidation on metal-oxide-coated Ti anodes: Kinetics, energy consumption and reaction mechanisms", *Chemosphere*, 163, pp. 584–591, 2016.
<https://doi.org/10.1016/j.chemosphere.2016.08.057>
- [24] Wang, G., Liu, Y., Ye, J., Lin, Z., Yang, X. "Electrochemical oxidation of methyl orange by a Magnéli phase Ti₄O₇ anode", *Chemosphere*, 241, 125084, 2020.
<https://doi.org/10.1016/j.chemosphere.2019.125084>
- [25] Zhou, C., Wang, Y., Chen, J., Niu, J. "Electrochemical degradation of sunscreen agent benzophenone-3 and its metabolite by Ti/SnO₂-Sb/Ce-PbO₂ anode: Kinetics, mechanism, toxicity and energy consumption", *Science of The Total Environment*, 688, pp. 75–82, 2019.
<https://doi.org/10.1016/j.scitotenv.2019.06.197>
- [26] Wang, C., Niu, J. F., Yin, L. F., Huang, J. X., Hou, L. A. "Electrochemical degradation of fluoxetine on nanotube array intercalated anode with enhanced electronic transport and hydroxyl radical production", *Chemical Engineering Journal*, 346, pp. 662–671, 2018.
<https://doi.org/10.1016/j.cej.2018.03.159>
- [27] Rathinakumaran, K., Meyyappan, R. M. "Electrochemical degradation of dye effluents using mixed oxide coated DSA electrode-a kinetic study", *International Journal of Chemical Science*, 13(3), pp. 1401–1409, 2015. [online] Available at: <https://www.tsjournals.com/articles/electrochemical-degradation-of-dye-effluents-using-mixed-oxide-coated-dsa-electrode-a-kinetic-study.pdf> [Accessed: 24 April 2023]
- [28] Ma, H., Wang, B., Luo, X. "Studies on degradation of Methyl Orange wastewater by combined electrochemical process", *Journal of Hazardous Material*, 149(2), pp. 492–498, 2007.
<https://doi.org/10.1016/j.jhazmat.2007.04.020>
- [29] Du, L., Wu, J., Qin, S., Hu, C. "Degradation mechanism of Methyl Orange by electrochemical process on RuOx–PdO/Ti electrode", *Water Science Technology*, 63(7), pp. 1539–1545, 2011.
<https://doi.org/10.2166/wst.2011.414>
- [30] Oguzie, K., Oguzie, E., Nwanonyi, S., Edoziem, J. K., Vrsalović, L. "Electrochemical decolorization of disperse blue-1 dye in aqueous solution", *Environmental Engineering Management Journal*, 20(9), pp. 1467–1476, 2021. [online] Available at: http://www.eemj.icpm.tuiasi.ro/pdfs/vol20/no9/Full/7_524_Oguzie_20.pdf [Accessed: 24 April 2023]
- [31] Gómez-Obando, V. A., García-Mora, A.-M., Basante, J. S., Hidalgo, A., Galeano, L.-A. "CWPO degradation of Methyl Orange at Circumneutral pH: Multi-Response Statistical Optimization, Main Intermediates and by-Products", *Frontiers in Chemistry*, 7, 772, 2019.
<https://doi.org/10.3389/fchem.2019.00772>
- [32] Kgatle, M., Sikhwivhilu, K., Ndlovu, G., Moloto, N. "Degradation Kinetics of Methyl Orange Dye in Water Using Trimetallic Fe/Cu/Ag Nanoparticles", *Catalysts*, 11(4), 428, 2021.
<https://doi.org/10.3390/catal11040428>
- [33] De Moura, D. C., Quiroz, M. A., Da Silva, D. R., Salazar, R., Martinez-Huitle, C. A. "Electrochemical degradation of Acid Blue 113 dye using TiO₂-nanotubes decorated with PbO₂ as anode", *Environmental Nanotechnology, Monitoring & Management*, 5, pp. 13–20, 2016.
<https://doi.org/10.1016/j.enmm.2015.11.001>
- [34] Jović, M., Stanković, D., Manojlović, D., Anđelković, I., Milić, A., Dojčinović, B., Roglić, G. "Study of the Electrochemical Oxidation of Reactive Textile Dyes Using Platinum Electrode", *International Journal of Electrochemical Science*, 8(1), pp. 168–183, 2013.
[https://doi.org/10.1016/S1452-3981\(23\)14011-9](https://doi.org/10.1016/S1452-3981(23)14011-9)